

## REVIEW

View Article Online

View Journal | View Issue



Check for updates

Cite this: *Org. Chem. Front.*, 2024, **11**, 4913

Received 19th May 2024,

Accepted 12th July 2024

DOI: 10.1039/d4qo00887a

rsc.li/frontiers-organic

Recent advancements in Ni/photoredox dual catalysis for  $\text{Csp}^3\text{--Csp}^3$  cross-coupling reactionsQi-Yun Huang<sup>a</sup> and Min Shi<sup>✉</sup> <sup>a,b</sup>

For the construction of  $\text{Csp}^3\text{--Csp}^3$  bonds, cross-coupling reactions in Ni/photoredox dual catalysis have recently achieved significant progress compared to traditional ones. In the past five years, a variety of free radical precursors have been developed to participate in redox neutral and reductive cross-coupling reactions via a dual photoredox/Ni-catalytic process. In this minireview, we mainly focus on the recent advancements (from 2019 to 2023) in Ni/photoredox dual catalysis for  $\text{Csp}^3\text{--Csp}^3$  cross-coupling reactions.

## 1. Introduction

The construction of carbon–carbon bonds is one of the core research topics in the field of organic chemistry.<sup>1</sup> A transition-metal-catalyzed cross-coupling reaction is one of the most effective methods to forge carbon–carbon bonds,<sup>1d</sup> and typical transition metal catalyzed cross-coupling reactions include the Kumada, Negishi, and Suzuki cross-coupling reactions. These reactions could produce  $\text{Csp}^2\text{--Csp}^2$  cross-coupling products very efficiently in the presence of a catalytic amount of transition metal under mild conditions. However, the formation of  $\text{Csp}^3\text{--Csp}^3$  bonds is usually difficult to achieve under these transition metal catalytic conditions due to the following factors:<sup>2</sup> (1) severe reaction conditions are required for the oxidative addition of more electron-rich  $\text{Csp}^3\text{--X}$  bonds with the transition metal and reductive elimination of the alkyl group from the metal center, (2) the  $\text{Csp}^3\text{--M}$  intermediate easily undergoes  $\beta\text{-H}$  elimination, affording alkene byproducts, and (3) alkyl halides are susceptible to base-assisted H–X elimination and halide exchange side reactions under cross-coupling conditions. In 2017, Fu and his co-workers summarized transition-metal-catalyzed alkyl–alkyl cross-coupling reactions,<sup>3</sup> demonstrating the initial progress of unactivated alkyl electrophilic reagents for  $\text{Csp}^3\text{--Csp}^3$  coupling, which also provided a key driving force for the development of Ni/photoredox dual catalysis.

Fortunately, odd-electron processes are not uncommon for nickel complexes. Thus, nickel species have abundant

and adjustable valence states ( $\text{Ni}^0/\text{Ni}^{\text{I}}/\text{Ni}^{\text{II}}/\text{Ni}^{\text{III}}/\text{Ni}^{\text{IV}}$ ).<sup>4a</sup> The reactivity of the Ni species is enriched by the availability of the  $\text{Ni}^{\text{I}}$  and  $\text{Ni}^{\text{III}}$  states as well as the possible involvement of radical processes.<sup>4b,c</sup> Moreover, under visible light irradiation, nickel is capable of undergoing single electron transfer (SET) smoothly, and the corresponding valence state will be raised or lowered by a single valence, making it more likely for free radicals to be generated mildly when exposed to light.<sup>4d,e,f</sup>

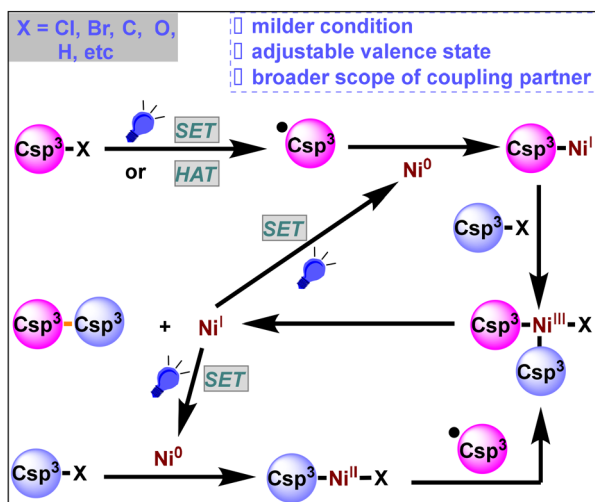
Traditional nickel-catalyzed coupling reactions involve three key steps:<sup>5a</sup> oxidative addition, transmetalation, and reductive elimination. Transmetalation is usually the decisive step in this type of reaction, with the exchange rate of different forms of carbon hybridization being  $\text{Csp} > \text{Csp}^2 > \text{Csp}^3$ , making the direct construction of  $\text{Csp}^3\text{--Csp}^3$  bonds particularly difficult.<sup>5b</sup> Owing to their radical-generating properties and abilities to modulate the oxidation state of metal catalysts,<sup>5c</sup> photocatalysts greatly broaden the range of electrophilic and nucleophilic reagents for cross-coupling reactions and are compatible with more reactive groups. Photocatalytic single-electron transmetalation is more suitable for  $\text{Csp}^3\text{--Csp}^3$  cross-coupling reactions than the conventional nickel-catalyzed transmetalation process using metal catalysis alone.

In recent years, the introduction of photocatalysts has expanded the range of coupling partners (such as  $\text{Csp}^3\text{--Cl}$  bonds,  $\text{Csp}^3\text{--Br}$  bonds,  $\text{Csp}^3\text{--C}$  bonds,  $\text{Csp}^3\text{--O}$  bonds,  $\text{Csp}^3\text{--H}$  bonds, *etc.*) and has greatly changed organic synthetic chemistry (Scheme 1). In this review, we summarize recent advancements in Ni/photoredox dual catalysis for  $\text{Csp}^3\text{--Csp}^3$  cross-coupling reactions over the last five years (2019–2023). We attempted to classify this context into three broad categories: neutral, reductive and oxidative cross-coupling according to the electrical properties of the coupling partners. Please note that some relevant information referred to can be found in the ESI section of the cited articles.

<sup>a</sup>Key Laboratory for Advanced Materials and Institute of Fine Chemicals, School of Chemistry & Molecular Engineering, East China University of Science and Technology, 130 Meilong Road, Shanghai 200237, China

<sup>b</sup>State Key Laboratory of Organometallic Chemistry, Center for Excellence in Molecular Synthesis, Shanghai Institute of Organic Chemistry, Chinese Academy of Sciences, 345 Ling-Ling Lu, Shanghai, 200032, China. E-mail: mshi@mail.sioc.ac.cn





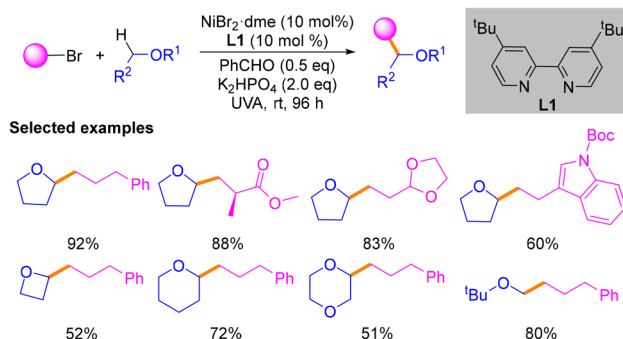
**Scheme 1** Ni/photoredox dual catalyzed cross-coupling reactions.

## 2. Redox neutral cross-coupling

Redox neutral cross-coupling is a reaction strategy of great importance in organic synthetic chemistry.<sup>6</sup> It is characterized by the design and selection of suitable reaction conditions so that the functional groups involved in the reaction do not undergo significant oxidation state changes during the course of the reaction, thereby improving the atom economy and selectivity of the reaction. In recent years, a number of redox neutral cross-coupling reactions under photoredox/nickel dual catalysis have been developed.

In 2019, according to the fact that triplet benzaldehyde excited using ultraviolet light can interact with hydrogen-donating solvents to produce  $\alpha$ -hydroxybenzyl and solvents such as tetrahydrofuran (THF) radicals as hydrogen atom transfer (HAT) catalysts possessing a strong ability to capture hydrogen, Hashmi and co-workers explored a platform for direct alkylation of  $\text{Csp}^3\text{-H}$  bonds with alkyl halides *via* a HAT process (Scheme 2).<sup>7</sup> The optimal reaction conditions are irradiation with UVA light,  $\text{NiBr}_2\cdot\text{dme}$  and **L1** as the nickel

**Hashmi's work, in 2019**

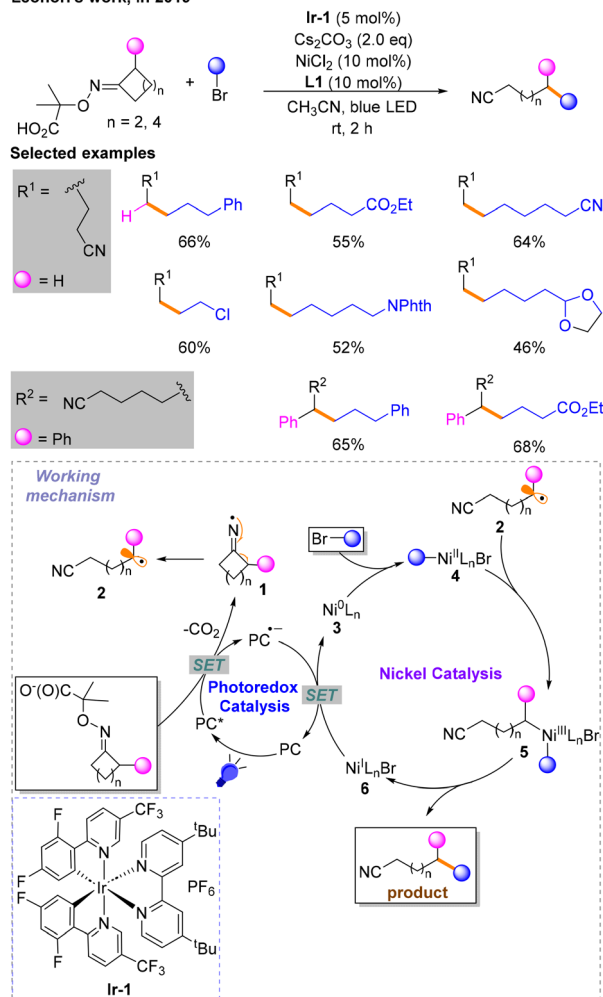


**Scheme 2**  $\text{Csp}^3\text{-Csp}^3$  cross-coupling reaction of alkyl bromides with ethers (Hashmi's work).

catalyst, benzaldehyde as both the photosensitizer and the HAT catalyst, and  $\text{K}_2\text{HPO}_4$  as the base. The substrate scope of bromide and ether coupling partners was investigated. However, the detailed mechanism requires more concrete study.

A few months later, Leonori and co-workers reported a divergent  $\text{Csp}^3\text{-Csp}^3$  coupling reaction *via* iminium radical ring opening in conjunction with nickel catalysis and photocatalysis, enabling remote alkylation of nitriles (Scheme 3).<sup>8</sup> The conditions for the highest yield are identified: **Ir-1** as the photocatalyst (PC),  $\text{Cs}_2\text{CO}_3$  as the base,  $\text{NiCl}_2$  with **L1** as the nickel catalytic system and  $\text{CH}_3\text{CN}$  as the solvent under blue LED irradiation. Single-electron oxidation and decarboxylation occur to provide radical **1** in the process of photocatalyst quenching in the excited state ( $\text{PC}^*$ ) to  $\text{PC}^{\bullet-}$ , followed by single-electron  $\beta$ -scission to give alkyl radical **2**. The nickel catalytic cycle begins with the oxidative addition of  $\text{Ni}^0$  species **3** with brominated hydrocarbon to produce  $\text{Ni}^{\text{II}}$  species **4**, followed by the addition of **2** generated in the photocatalytic

**Leonori's work, in 2019**



**Scheme 3** Coupling reaction of iminium radical ring-opening in conjunction with Ni-catalysis.

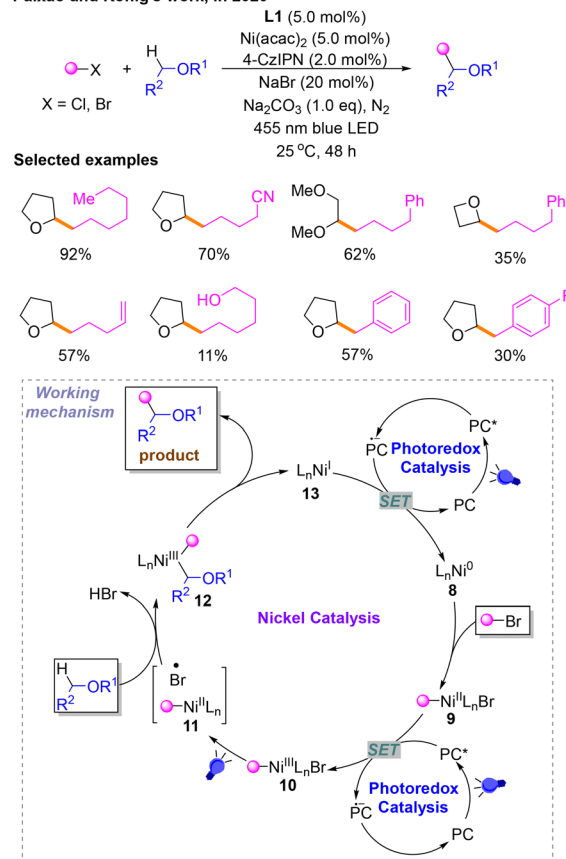


stage to give  $\text{Ni}^{\text{III}}$  species **5**, and finally reductive elimination to obtain a  $\text{Csp}^3\text{-Csp}^3$  coupling product. The  $\text{Ni}^{\text{I}}\text{Br}$  **6** generated from the above process is reduced to **3**, and  $\text{PC}^{\text{--}}$  is oxidized to PC simultaneously *via* a SET process.

Two months later, a method using 4-alkyl-1,4-dihydropyridines (DHPs) with oxa- and azabenzonorbornadienes to construct  $\text{Csp}^3\text{-Csp}^3$  architectures was developed by Molander's group (Scheme 4).<sup>9</sup> Notably, the regioselective and diastereoselective *cis*-1,2-dihydro-1-naphthyl alcohol backbone's structure can be achieved through this cross-coupling process under a nickel/photoredox dual catalytic system. The best conditions for the reaction are 4-CzIPN as the PC,  $\text{NiCl}_2\cdot\text{dme}$  with **L2** or **L3** as the nickel catalytic system, and acetone as the solvent under blue LED irradiation. A series of mechanistic experiments have proven the impossible activation of the substrate by by-products and the product-determining-step involving no benzyl residues. According to density functional theory (DFT) calculations, in this program, a  $\pi\text{-}\sigma$  isomerization process was believed to occur in  $\text{Ni}^{\text{III}}$  species **7**. The Curtin-Hammett principle supported the product produced with 1,2-regioselectivity.

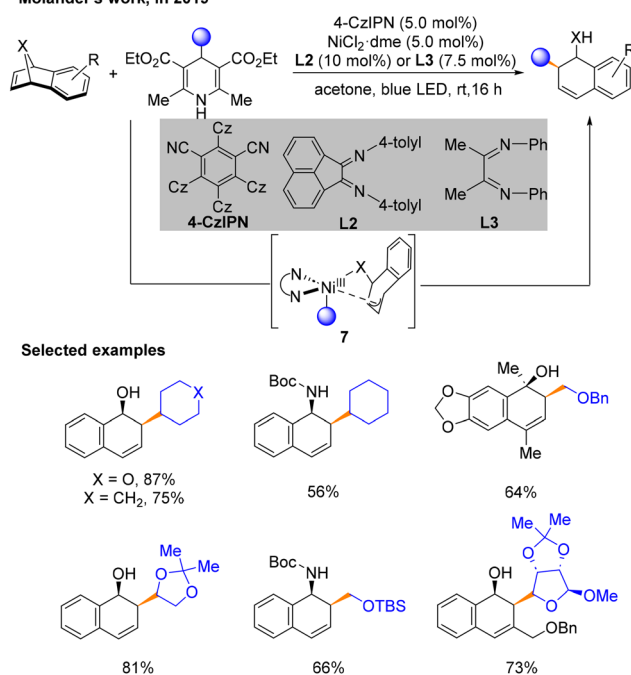
In 2020, taking into account the previously mentioned study of other researchers, a protocol was introduced for a  $\text{Csp}^3\text{-Csp}^3$  cross-coupling reaction of alkyl bromides with ethers using a Ni/photoredox dual catalyst *via* a halide-mediated HAT process by Paixão and König (Scheme 5).<sup>10</sup> In this platform, they used 4-CzIPN as the photocatalyst to optimize the reaction conditions, and it is determined that the reaction should be carried out upon irradiation with a blue

#### Paixão and König's work, in 2020



**Scheme 5**  $\text{Csp}^3\text{-Csp}^3$  cross-coupling reaction of alkyl bromides with ethers (Paixão and König's work).

#### Molander's work, in 2019

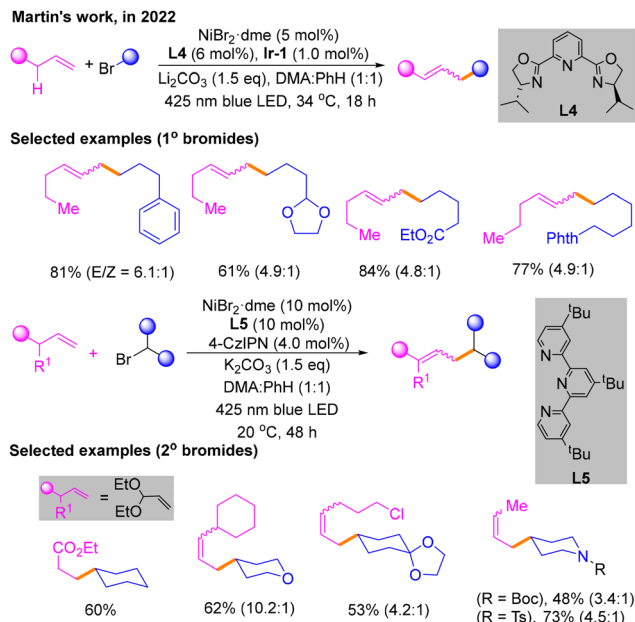


**Scheme 4** Cross-coupling of oxa- and azabenzonorbornadienes with DHP (Molander's work).

LED in the presence of  $\text{Na}_2\text{CO}_3$  using  $\text{Ni}(\text{acac})_2$  and **L1** as the catalyst and 4-CzIPN as the photosensitizer in THF. The catalytic cycle begins with the oxidative addition of the  $\text{Ni}^0$  species **8** with a bromoalkane substrate to obtain the  $\text{Ni}^{\text{II}}$  species **9**. Then, **9** is oxidized to afford  $\text{Ni}^{\text{III}}$  **10** by  $\text{PC}^*$  to deliver  $\text{PC}^{\text{--}}$ . Subsequently, **10** absorbs visible light, generating the  $\text{Ni}^{\text{II}}$  species **11** and a halogen radical as a HAT agent. The generation of alkyl radicals is caused by the HAT of substrate ether and captured by **11** to provide **12**. This HAT process is induced by the bromine radicals produced by the homolysis of the Ni-Br bond from **10** under the irradiation of a blue LED. The product comes from the reductive elimination of **12**. Finally,  $\text{Ni}^{\text{I}}$  species **13** derived from **12** is reduced to  $\text{Ni}^0$  **8** by  $\text{PC}^{\text{--}}$  to deliver the PC, which makes the catalytic cycle complete.

After that, combining a light-induced system with nickel catalysis, redox-neutral and site-selectivity  $\text{Csp}^3\text{-H}$  alkylation of an unactivated  $\alpha$ -olefin with an alkyl bromide was reported by Martin's group in 2022 (Scheme 6).<sup>11</sup> The reaction is able to obtain the maximum yield of primary alkyl bromides under blue LED irradiation, with  $\text{NiBr}_2\cdot\text{dme}$  and **L4** as the nickel catalytic system, **Ir-1** as the photocatalyst of light,  $\text{K}_2\text{CO}_3$  as the base, and dimethylacetamide (DMA):PhH (1:1) as the solvent. Surprisingly, the optimal conditions of secondary



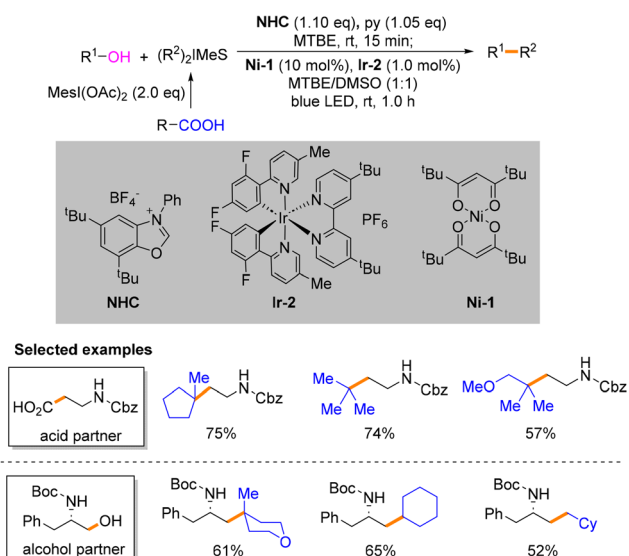


**Scheme 6** Csp<sup>3</sup>-H alkylation of an unactivated  $\alpha$ -olefin.

bromide hydrocarbons are not exactly the same in ligands and photocatalysts. For secondary bromides, **L5** is the best ligand with 4-CzIPN as the photocatalyst.

Soon after, MacMillan and co-workers developed a strategy for photo- and nickel-catalyzed Csp<sup>3</sup>-Csp<sup>3</sup> cross-coupling reactions involving N-heterocyclic carbene (NHC)-mediated deoxygenation of alcohols and hypervalent iodine-mediated decarbonylation of carboxylic acids (Scheme 7).<sup>12</sup> Methyl tertiary butyl ether (MTBE):dimethyl sulfoxide (DMSO) (1:1) is used as the solvent. Different from previously reported schemes, the two Csp<sup>3</sup> radicals involved in the reaction are both generated

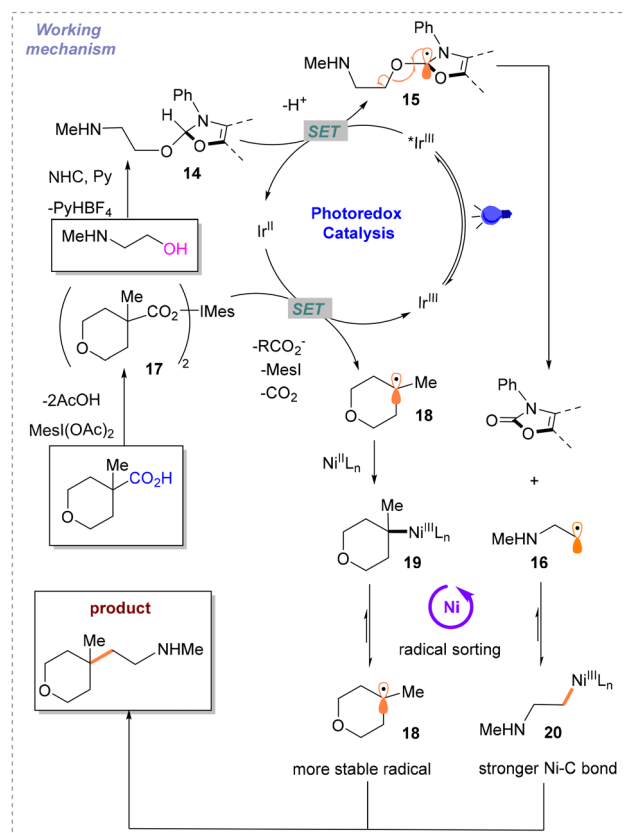
**MacMillan's work, in 2022**



**Scheme 7** Cross-coupling reaction of alcohols and carboxylic acids.

during the photocatalytic SET process. In this event, the alcohol substrate reacts with NHC to afford the product **14**, which can undergo SET with <sup>\*</sup>Ir<sup>III</sup>. The resulting intermediate **15** undergoes the process of  $\beta$ -breakage to generate radical **16**. Carboxylic acids are activated by iodine hypervalent to give **17**. Ir<sup>II</sup> then undergoes SET with **17** to generate another free radical **18** and Ir<sup>III</sup>. To maintain the catalytic cycle, blue light irradiation excites Ir<sup>III</sup> to <sup>\*</sup>Ir<sup>III</sup>. The difficulty of this strategy is distinguishing between the two different free radicals **16** and **18** generated instantaneously. To solve this problem, based on the difference in the relative instability of the highly substituted metal-alkyl species and different strengths of nickel-carbon bonds, a radical sorting method was conceived. That is, **20** is more stable than **19**, but their radical stabilities are the opposite with radical **18** being more stable than radical **16** (Scheme 8). After verifying the practicality of this idea, the author explored its generality with primary, secondary, and tertiary alkyl acids and alcohols under the optimal conditions.

Two months later, a platform for cross-coupling mediated by Ni and a photocatalyst is developed by Martin's group to build Csp<sup>3</sup>-Csp<sup>3</sup> bonds utilizing dihydroquinazolinones derived from ketones (Scheme 9).<sup>13</sup> In this metal and photocatalyst dual catalytic system, the Ni and photo-induced catalytic cycle is similar to that discussed previously. Haloalkane substrates produce Ni<sup>II</sup> species **21** in the Ni catalytic cycle.

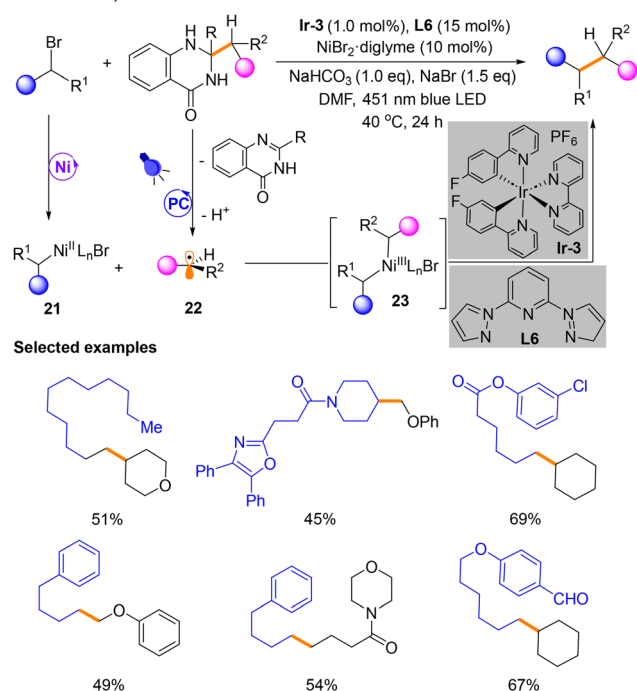


**Scheme 8** Proposed reaction design of cross-coupling reactions of carboxylic acids with alcohols.





## Martin's work, in 2022

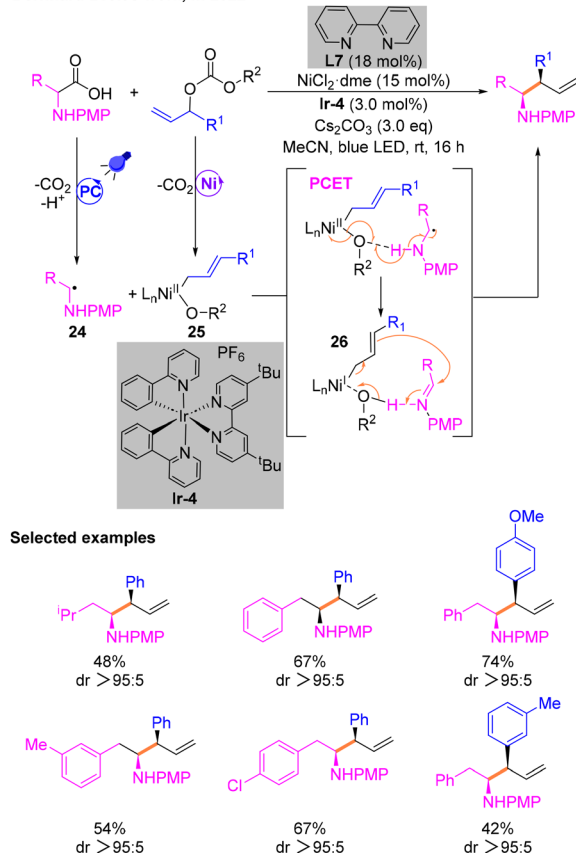


**Scheme 9** Csp<sup>3</sup>–Csp<sup>3</sup> cross-coupling reaction of dihydroquinazolinones with bromoalkanes.

Alkyl radicals **22** are produced by the substrate dihydroquinazolinone in the photocatalytic phase. Then, **21** and **22** could undergo radical recombination to generate Ni<sup>III</sup> species **23**. The product is also obtained by the reductive elimination of **23**. However, a distinguishing feature of this reaction is that the dihydroquinazolinone serves as a radical source causing  $\alpha$  C–C cleavage through aromatization, which is induced by single-electron oxidation of photocatalysis. The selected examples have also been shown in Scheme 9.

Soon after, Breit and co-workers exploited a way for the construction of homoallyl amines utilizing  $\alpha$ -amino acids *via* photoredox Ni-catalytic cross-coupling (Scheme 10).<sup>14</sup> This reaction enables the functionalization of allyl groups and diastereoselectively obtains branched allylation products involving  $\alpha$ -amino radical intermediates. The first investigation was conducted using model substrates and determined the most optimal conditions: NiCl<sub>2</sub>·dme and **L7** as the metal catalytic system, Cs<sub>2</sub>CO<sub>3</sub> as the base, and [Ir(ppy)<sub>2</sub>(dtbbpy)]PF<sub>6</sub> (**Ir-4**) as the PC. Subsequently, the arylallyl electrophile substrate was expanded using *N*-phenyl or *N*-*p*-methoxyphenyl (PMP) phenylalanine as the  $\alpha$ -amino radical precursor. Mechanistic experiments illustrated that the free radicals involved in the catalytic cycle are generated by SET in the photocatalytic cycle and then decarboxylation. The diastereoselectivity of products was explained by DFT calculations. A critical step is the proton coupled electron transfer (PCET) process of the radical **24** and Ni<sup>II</sup> species **25** to afford **26**. Then, **26** in combination with the allyl group undergoes a nucleophilic attack on the imine to give the desired product.

## Bernhard Breit's work, in 2022

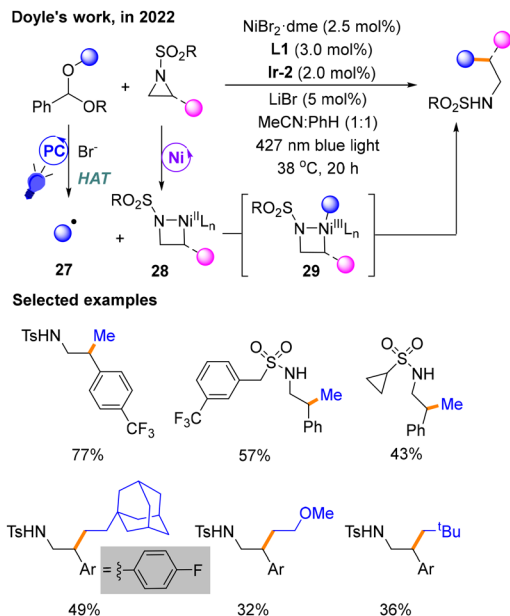


**Scheme 10** Synthesis of homoallyl amines by a cross-coupling reaction.

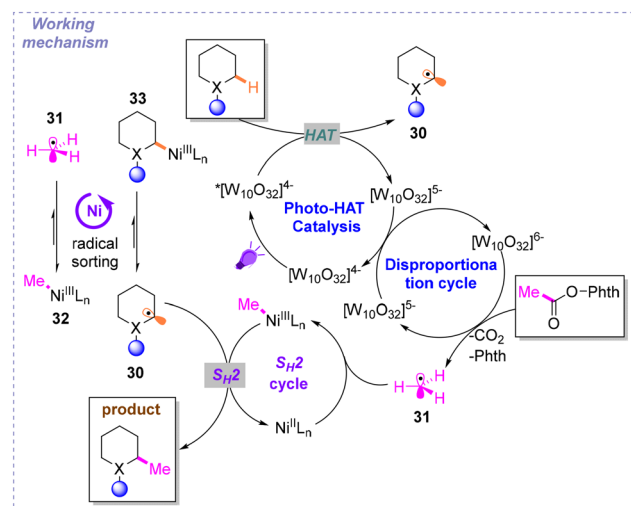
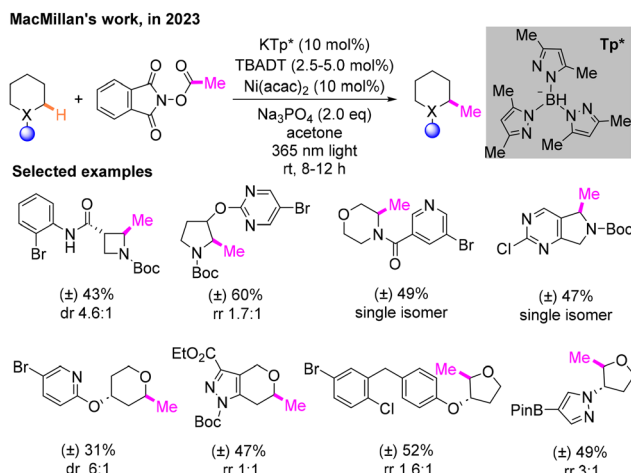
A few months later, Doyle's group utilizing benzaldehyde dialkyl acetals derived from alcohols developed a method for Csp<sup>3</sup>–Csp<sup>3</sup> cross-coupling reactions with aziridines (Scheme 11).<sup>15</sup> The product is obtained with NiBr<sub>2</sub>·dme and **L1** as the nickel catalytic system using **Ir-2** as the PC under blue light exposure in MeCN:PhH (1 : 1) mixed solvent. The function of the additive LiBr is to stabilize the anionic sulfonamide and facilitate the release of the product. Benzaldehyde dialkyl ketals are employed by HAT to produce radical species **27** under the stimulation of a photocatalyst and bromide ions. Mechanistic studies show that the activation of dialkyl acetals *via* HAT by Br<sup>−</sup> happens during the photocatalytic phase to give **27**, and the oxidative addition of aziridines occurs in the Ni catalytic cycle to afford **28**, explaining the differential activation of the two coupling partners. The product is released by the reductive elimination reaction from Ni<sup>III</sup> species **29**.

Then, inspired by the Csp<sup>3</sup>-methyl group catalyzed by radical *S*-adenosylmethionine (SAM) methyltransferase in biological systems and some previous work, MacMillan and co-workers reported a Csp<sup>3</sup>–Csp<sup>3</sup> coupling reaction through radical sorting and bimolecular homolytic substitution (S<sub>H</sub>2), in which direct methylation occurs on saturated heterocyclic Csp<sup>3</sup>–H bonds (Scheme 12).<sup>16</sup> The most ideal conditions are irradiation under 365 nm light, Ni(acac)<sub>2</sub>·KTP\* as the metal





**Scheme 11** Csp<sup>3</sup>–Csp<sup>3</sup> cross-coupling reaction of benzaldehyde dialkyl acetals with aziridines.

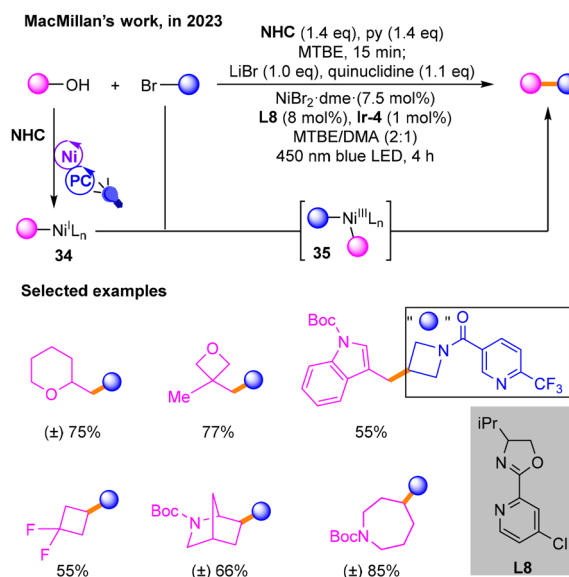


**Scheme 12** Methylation of saturated heterocyclic Csp<sup>3</sup>–H bonds.

catalyst, Na<sub>3</sub>PO<sub>4</sub> as the base and tetrabutylammonium decatungstate (TBADT) as the HAT reagent and photocatalyst in acetone. The universality of this strategy is also assessed. These two alkyl radicals are respectively produced by HAT and decarboxylation in the photocatalytic cycle. The excited triplet state of decatungstate <sup>\*</sup>[W<sub>10</sub>O<sub>32</sub>]<sup>4–</sup> under light undergoes a HAT process at the hydridic α-amino C–H bond of the first substrate, resulting in reduced [W<sub>10</sub>O<sub>32</sub>]<sup>5–</sup> as well as alkyl radical **30**. Another radical **31** is produced during the disproportionation cycle from the second substrate. Key to the success of this mechanism is the previously mentioned radical sorting effect mediated by nickel. Radicals **30** and **32** are more stable than **31** and **33**, respectively. In addition, products are obtained from the S<sub>H</sub>2 process.

In 2023, Macmillan<sup>17</sup> used NHC to activate alcohols and performed coupling reactions with brominated hydrocarbons to build Csp<sup>3</sup>–Csp<sup>3</sup> bonds (Scheme 13). In the photocatalytic cycle, the alcohols are activated by NHC-mediated C–O homolysis to produce alkyl radicals, which is similar to their previous reports. Then, the resulting Ni<sup>I</sup> species **34** during nickel and photo-induced catalysis undergoes oxidative addition with halogenated hydrocarbons to produce Ni<sup>III</sup> species **35**, and finally the target product is obtained through reductive elimination of **35**.

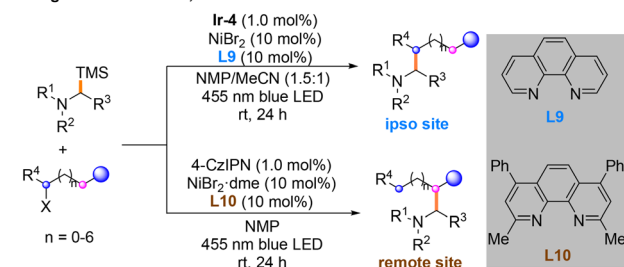
Later, a light/nickel-catalyzed Csp<sup>3</sup>–Csp<sup>3</sup> cross-coupling reaction of α-silylamines with unactivated alkyl halides, which could occur on the *ipso* and remote sites of alkyl halides selectively through ligand regulation, was for the first time described by Huang and Yuan in 2023 (Scheme 14).<sup>18</sup> They found that photosensitizer **Ir-4** is the most suitable for the *ipso*-site reaction, and 4-CzIPN is best for the remote-site reaction. After careful screening of the reaction conditions. α-N-



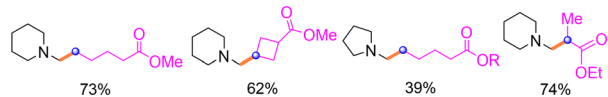
**Scheme 13** The cross-coupling reaction of activated alcohols with NHC and brominated hydrocarbons.



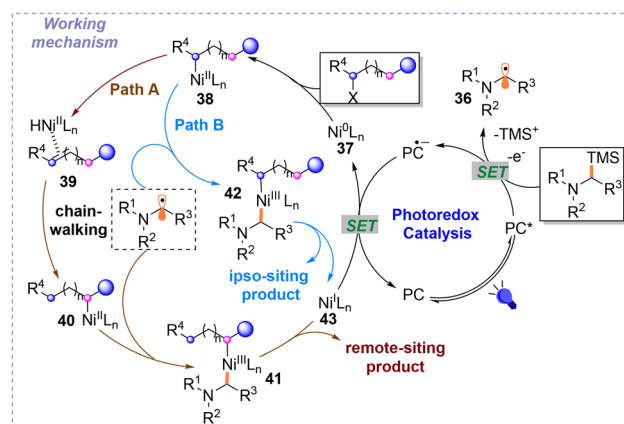
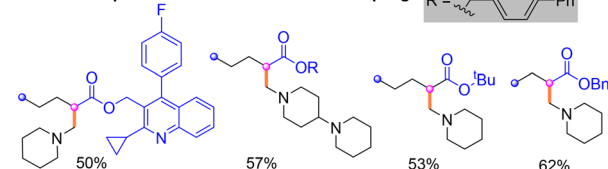
## Huang and Yuan's work, in 2023



## Selected examples of ipso-selective cross-coupling



## Selected examples of remote-selective cross-coupling

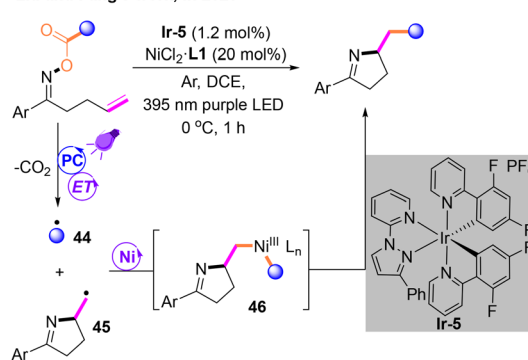


**Scheme 14** Csp<sup>3</sup>–Csp<sup>3</sup> cross-coupling reaction of  $\alpha$ -silylamine with alkyl bromides.

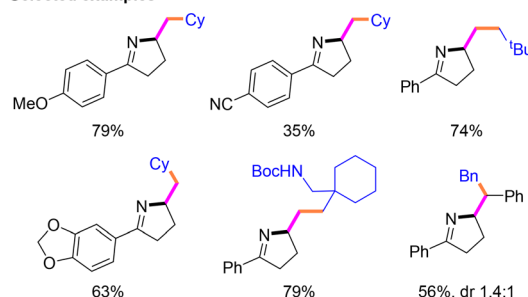
Alkyl radicals participating in the nickel catalytic cycle are generated during the photocatalytic cycle. When L9 is used as the ligand, the olefin substrate will isomerize to form the *ipso*-site product (Path A). Moreover, the remote-site product can be output when the ligand is L10 (Path B). Remote- and *ipso*-site products are obtained from different Ni<sup>III</sup> species: 41 and 42. Mechanistic experiments have shown that  $\beta$ -hydrogen is necessary for the generation of remote-site products during the chain-walking process. DFT calculations proved that the steric hindrance of ligands is a factor affecting site selectivity.

After that, Liu and Fang reported a new Csp<sup>3</sup>–Csp<sup>3</sup> cross-coupling system through decarboxylation<sup>19</sup> mediated by a PC and the subsequent coupling of two radicals by a nickel catalyst (Scheme 15). This reaction was performed under the irradiation of a purple LED with dichloroethane (DCE) as the solvent, unlike most reactions that use a blue LED as the light source. Both radicals 44 and 45 are generated *via* an energy

## Liu and Fang's work, in 2023



## Selected examples

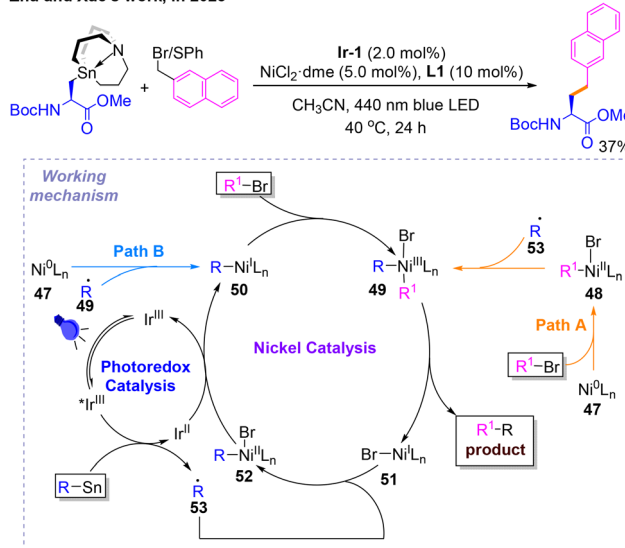


**Scheme 15** Csp<sup>3</sup>–Csp<sup>3</sup> decarboxylated cross-coupling reaction via E<sub>T</sub>.

transfer (E<sub>T</sub>) process during the photocatalytic stage, followed by a nickel-mediated cross-coupling reaction to afford Ni<sup>III</sup> species 46. The reductive elimination of 46 occurs to produce the target product.

Subsequently, a photonic nickel-cocatalyzed Stille coupling reaction was developed by Zhu and Xue (Scheme 16).<sup>20</sup> After determining the reaction conditions for Csp<sup>2</sup>–Csp<sup>3</sup> coupling,

## Zhu and Xue's work, in 2023

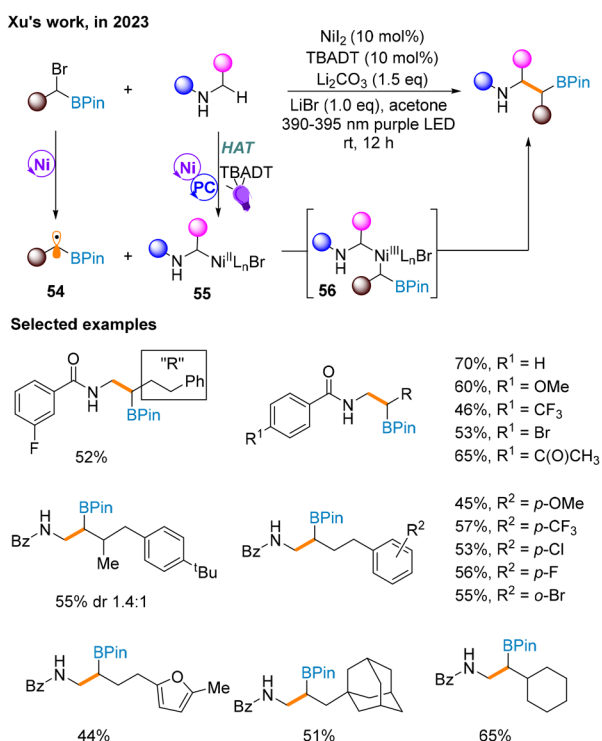


**Scheme 16** Photo- and nickel-catalyzed Stille coupling reaction.



the author evaluated the scope of this protocol, in which only a  $\text{Csp}^3\text{-Csp}^3$  coupling product was reported. Several mechanistic studies and DFT calculations were carried out to show how this reaction proceeds. There are two pathways A and B for this reaction. The difference between them is whether conventional oxidative addition occurs first to give **48** followed by single-electron oxidative addition to give **49** (Path A), or whether the opposite occurs to give **50**, followed by **49** (Path B). The products and  $\text{Ni}^{\text{I}}$  species **51** of both pathways are obtained by reductive elimination of  $\text{Ni}^{\text{III}}$  species **52**. Radical **53** could be captured by **51** to get **52**, which would be reduced to **50**.

A month later, a  $\text{Csp}^3\text{-Csp}^3$  cross-coupling reaction of  $\alpha$ -bromoboronates and  $\beta$ -amino boronates through C–H bond activation is reported by Xu and co-workers to forge  $\beta$ -amino boronates (Scheme 17),<sup>21</sup> whose synthesis is currently rare. It is worth noting that the additional use of ligands will decrease the yield, and thus this strategy does not involve supernumerary ligands. In addition, unlike most of the above methods, this strategy uses the irradiation of purple light to maintain the catalytic cycle. Mechanistically,  $\alpha$ -bromoboronate undergoes a one-electron redox reaction in nickel catalysis to produce  $\alpha$ -borate radical **54**. The  $\alpha$ -*N*-alkyl radical produced by the photocatalytic cycle *via* the HAT process is captured by the Ni catalytic cycle to afford  $\text{Ni}^{\text{II}}$  species **55** and then combined with **54**. Finally, the product is obtained through reductive elimination of  $\text{Ni}^{\text{III}}$  species **56**.

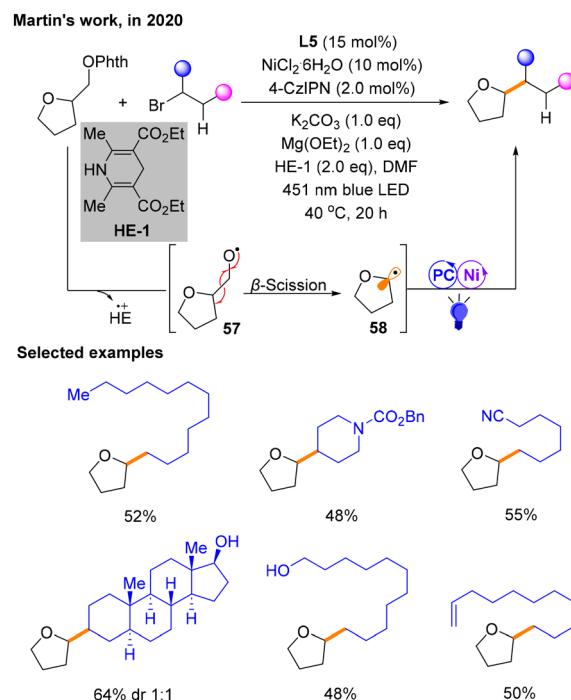


**Scheme 17** Synthesis of  $\beta$ -amino boronates *via* a  $\text{Csp}^3\text{-Csp}^3$  cross-coupling reaction.

### 3. Reductive cross-coupling

Reductive cross-coupling reactions are also an important class of reactions in organic chemistry.<sup>22</sup> Reactants usually undergo electron transfer and recombination of chemical bonds in the presence of a reducing agent. In this reaction, a reducing agent is used to facilitate the formation of new carbon–carbon bonds between different organic fragments. In recent years, there have been a number of reductive coupling reactions under photoredox/nickel dual catalysis.

In 2020, Martin and co-workers demonstrated the successful development of a dual photoredox/Ni-catalytic process that gives access to alkylation of  $\text{Csp}^3$  *via*  $\beta$ -scission of a special class of aliphatic alcohol derivatives, *N*-phthalimide ethers (Scheme 18).<sup>23</sup> Specifically, utilizing 4-CzIPN as the PC,  $\text{K}_2\text{CO}_3$  as the base, Hantzsch ester (HE-1) as the electron donor (ED) and  $\text{NiCl}_2\cdot\text{L5}$  as the metal catalyst under the irradiation of blue light, a series of  $\text{Csp}^3\text{-Csp}^3$  coupling structures were produced. The range of  $\text{Csp}^3$  alkylation was studied, explaining the influence of ligand denticity. Some examples are selected and shown in Scheme 18. In this protocol, HE-1 is not only able to reduce *N*-phthalimide ethers (Ophth) to provide radicals **57**, but it can also maintain the photocatalytic cycle. The photocatalytic cycle does not generate **57** involved in coupling, but **57** is generated by HE. Subsequently, the  $\beta$ -breakage of **57** occurs through the single electron activity of the ether with  $\text{HE}^+$ , generating alkyl radical species **58** that participate in the nickel and photocatalytic cycle to afford the product. In addition, the authors suggest that there may be an electron-



**Scheme 18** Cross-coupling reaction of  $\text{sp}^3$  alkylation *via*  $\beta$ -scission of *N*-phthalimide ethers.



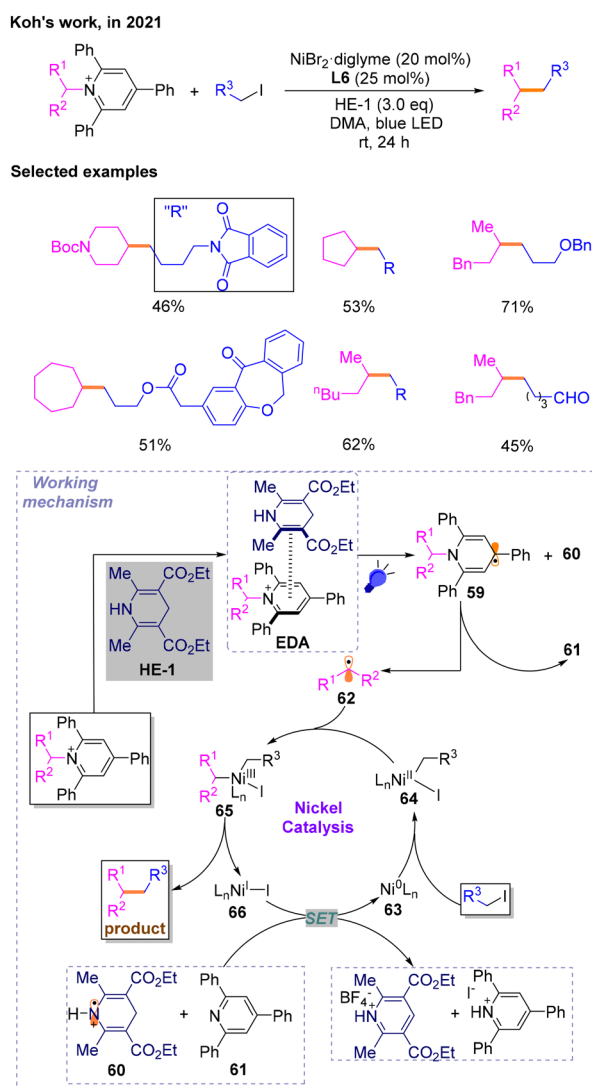


donor-acceptor (EDA) complex between HE and the substrate prior to  $\beta$ -scission.

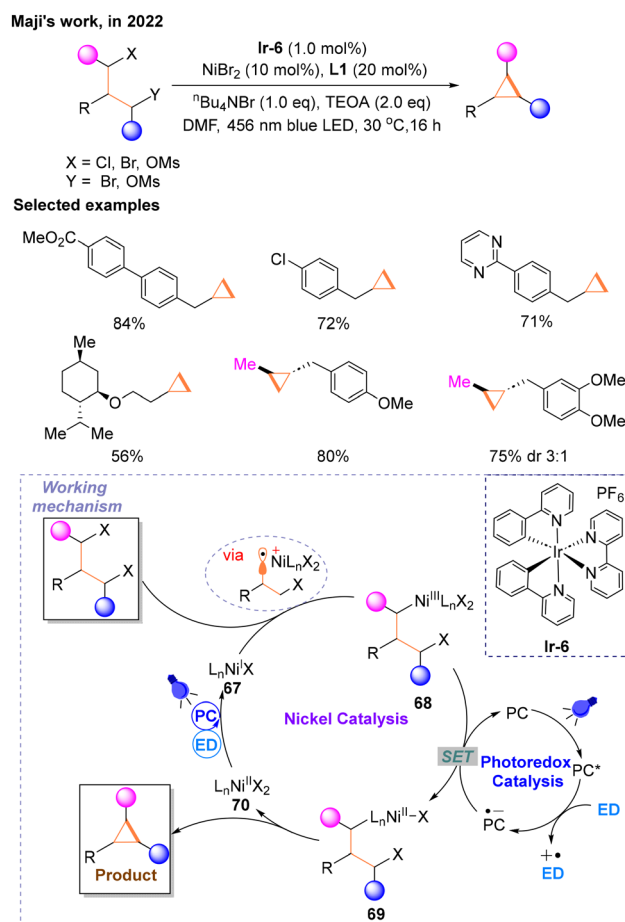
A year later, affected by the redox active characteristics of *N*-alkylpyridinium salts, a technology for constructing a  $\text{Csp}^3$ - $\text{Csp}^3$  skeleton *via* a photo-induced and nickel-catalyzed cross-electrophile coupling reaction with *N*-alkylpyridinium salts as radical precursors was disclosed by Koh in 2021 (Scheme 19).<sup>24</sup> After optimization studies, the author explored the substrate range of deamination alkylation reactions with bromides and iodides, respectively, and found that the iodides could perform  $\text{Csp}^3$ - $\text{Csp}^3$  cross-coupling reactions effectively. Then, several mechanistic experiments were conducted, and it is believed that the proposed mechanism may involve EDA complexes formed between *N*-alkylpyridinium salts and HE-1. Then, photoexcitation and SET occur to generate dihydropyridine radicals **59** and  $\text{HE}^{+}$  **60**, followed by deamination cleavage triggered by aromatization to produce triphenylpyridine

**61** and alkane radical **62** involved in the catalytic cycle. The species **60** and **61** will reduce  $\text{Ni}^{\text{I}}$  **66** to  $\text{Ni}^0$  **63**. **63** would then undergo an oxidative addition reaction with halogenated hydrocarbons to produce  $\text{Ni}^{\text{II}}$  **64**, which could capture the previously generated alkyl radicals **62** affording  $\text{Ni}^{\text{III}}$  species **65**. To complete the catalytic cycle, reductive elimination of **65** occurs to produce the desired products and **66**.

In 2022, Maji and co-workers proved that metallaphotoredox catalysis can be a prominent strategy to make the cyclopropane ring *via* an intramolecular  $\text{Csp}^3$ - $\text{Csp}^3$  cross-electrophile coupling reaction (Scheme 20) of 1,3-alkyl electrophiles.<sup>25</sup> The reaction conditions were optimized using primary alkyl 1,3-dimesylate with an ester functionality as a model substrate, and the optimal reaction conditions were finally determined: **Ir-6** as the PC,  $\text{NiBr}_2$  with **L1** as the transition metal catalyst,  $^t\text{Bu}_4\text{NBr}$  as the additive, triethanolamine (TEOA) as the ED, *N,N*-dimethylformamide (DMF) as the solvent and the reaction was performed at room temperature under the irradiation of a blue LED. In addition, secondary alkyl electrophiles could also react smoothly when one of the halogen atoms in the substrate is replaced with OMs. As the author speculated,  $\text{PC}^*$  was quenched to  $\text{PC}^{\cdot-}$  by the ED. The nickel catalytic cycle starts



**Scheme 19** The coupling reaction involving *N*-alkylpyridinium salts as radical precursors.



**Scheme 20** Synthesis of cyclopropanes *via* an intramolecular  $\text{Csp}^3$ - $\text{Csp}^3$  cross-coupling reaction.

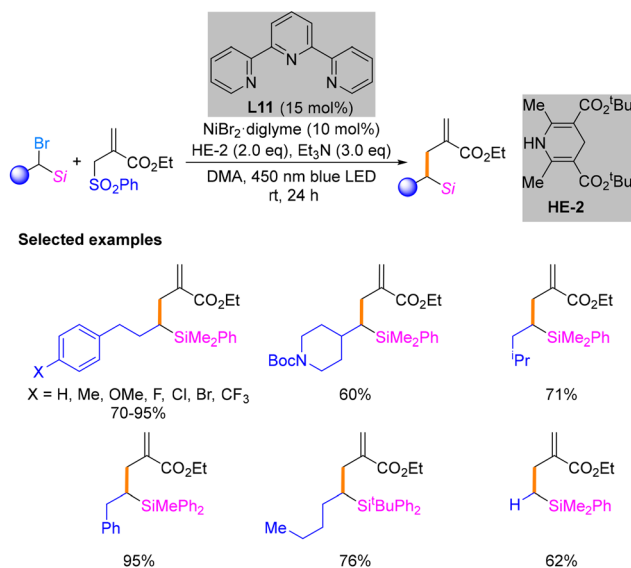


with  $\text{Ni}^{\text{I}}$  **67** generated from a photocatalytic SET involving the ED, undergoing oxidative addition with halogenated hydrocarbons *via* a radical process to form  $\text{Ni}^{\text{III}}$  **68**, which is subsequently reduced to  $\text{Ni}^{\text{II}}$  **69** by  $\text{PC}^{\text{--}}$  delivering the PC.  $\text{PC}^{\text{--}}$  is regenerated under the blue light irradiation and ED to complete the photocatalytic cycle. Subsequently, **69** undergoes oxidative addition and reductive elimination to produce the target product. The new  $\text{Ni}^{\text{II}}$  species **70** produced in this step undergoes the same photocatalytic process and is reduced to  $\text{Ni}^{\text{I}}$  **67** to enter the next catalytic cycle.

Later, Oestreich's research group achieved a reductive cross-coupling reaction between  $\alpha$ -silylated alkyl bromides and an allylic sulfone using a HE as the reducing agent in 2022 (Scheme 21).<sup>26</sup> It has been experimentally verified that the key to the successful conduction of the reaction is the ability of the methylsilane at the  $\alpha$ -position of the alkyl bromide to stabilize the carbon radicals. After conditional screening, it is determined that the most qualified conditions are  $\text{NiBr}_2$ -diglyme as the nickel precatalyst and terpyridine **L11** as the ligand as well as HE-2 and  $\text{Et}_3\text{N}$  under irradiation with a blue LED in DMA as the solvent. The reaction scope of this coupling reaction was subsequently evaluated under these conditions. Notably, this process does not require a photocatalyst but only blue light irradiation to maintain the catalytic cycle. Thus, further study is needed to gain mechanistic insights.

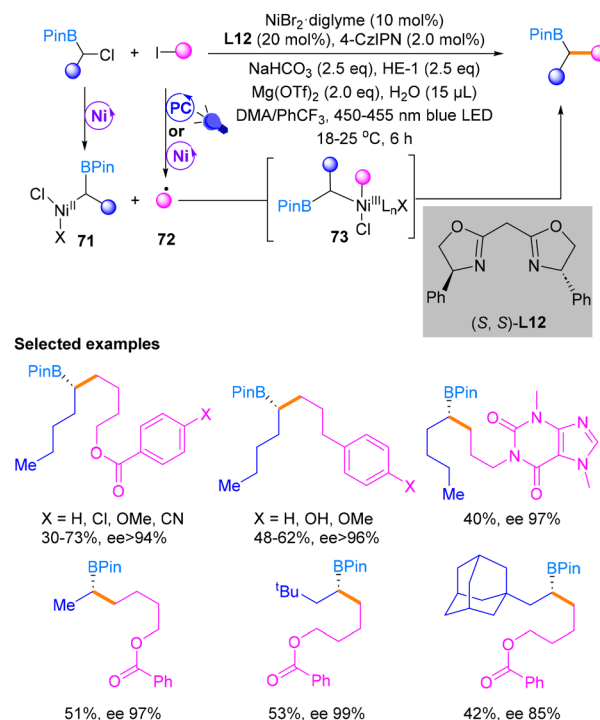
In 2023, Xu and co-workers described  $\text{Csp}^3$ - $\text{Csp}^3$  cross-coupling with dual Ni/photocatalysis utilizing unactivated alkyl halides and racemic  $\alpha$ -chloroboronates as substrates (Scheme 22).<sup>27</sup> This strategy enables the highly selective synthesis of chiral secondary alkylborates, important intermediates in organic synthesis, making it possible to rapidly construct enantiomerically enriched complex molecules.

#### Oestreich's work, in 2022



**Scheme 21** Cross-coupling reaction of  $\alpha$ -silylated alkyl bromides and an allylic sulfone.

#### Xu's work, in 2023



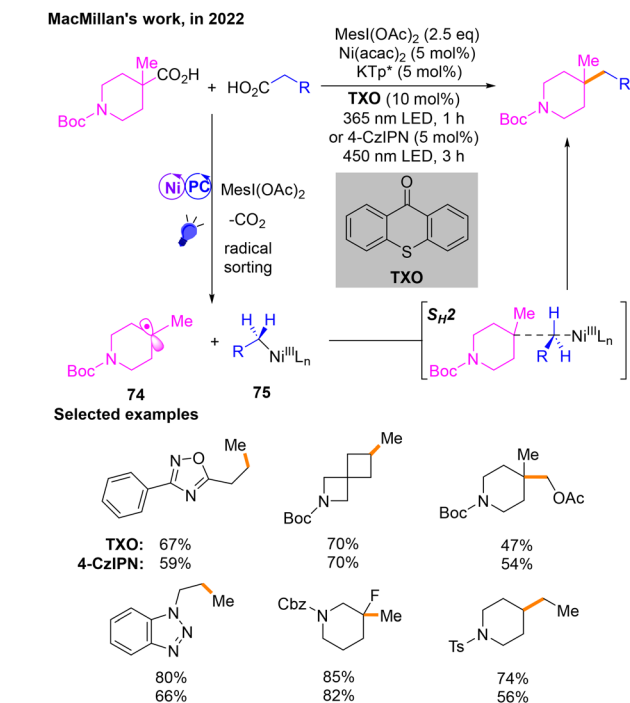
**Scheme 22** Cross-coupling of  $\alpha$ -chloroboronates with alkyl iodides.

This reaction could achieve the highest yield in the  $\text{NiBr}_2$ -diglyme catalytic system using 4-CzIPN as the PC and  $\text{DMA}:\text{PhCF}_3$  (1 : 1) as the solvent in the presence of some additives. Then, the substrate scope of  $\alpha$ -chloroboronates and alkyl iodides for reductive cross-coupling was expanded. Based on radical-clock reactions and other mechanistic verification experiments, the author proposed that a  $\text{Csp}^3$  radical was formed in the photocatalytic stage from alkyl iodides under the irradiation of blue light. In addition,  $\alpha$ -chloroboronates are activated in the nickel catalytic cycle to afford  $\text{Ni}^{\text{II}}$  species **71**. Subsequently, free radical addition and reductive elimination with **72** occur successively to generate the final product through the  $\text{Ni}^{\text{III}}$  species **73**. HE-1 also acts as the ED to maintain the photocatalytic cycle.

## 4. Oxidative cross-coupling

Oxidative cross-coupling offers a new approach for constructing C-C bonds.<sup>28a</sup> In this type of reaction, transition-metal catalysts and oxidants are usually utilized to induce cross-coupling of two different nucleophilic organic molecules,<sup>28b,c</sup> resulting in the formation of new carbon-carbon or carbon-hetero bonds. In recent years, the construction of  $\text{Csp}^3$ - $\text{Csp}^3$  bonds by oxidative cross-coupling has been greatly developed, especially in the field of electrocatalysis.<sup>28d</sup> However, with regard to Ni/photoredox dual catalysis, there are limited cases of  $\text{Csp}^3$ - $\text{Csp}^3$  bond construction in oxidative cross-coupling.





**Scheme 23** Decarboxylative cross-coupling of aliphatic acids.

In 2022, a decarboxylative Csp<sup>3</sup>-Csp<sup>3</sup> cross-coupling reaction<sup>29</sup> of aliphatic acids was developed by MacMillan's group (Scheme 23). The two free radicals of this reaction are produced after the corresponding aliphatic carboxylic acid substrates are activated by MesI(OAc)<sub>2</sub>. Then radical **74** and Ni<sup>III</sup> species **75** are produced during the radical sorting process, and they finally produce the target product through S<sub>H2</sub>. When thioxanthone (TXO) is used as the photosensitizer, the reaction can occur under 365 nm violet light irradiation, and it is worth noting that when the photosensitizer is changed to 4-CzIPN, the product can also be obtained under the irradiation of a 450 nm blue LED. In addition, MesI(OAc)<sub>2</sub> acts as the oxidant in this reaction.

## 5. Conclusion and outlook

This minireview mainly covers the research on Ni/photoredox dual catalyzed Csp<sup>3</sup>-Csp<sup>3</sup> cross-coupling reactions from 2019 to 2023. Under clean and mild light irradiation conditions and cheap nickel metal catalysis, various compounds containing C-C structures can be easily obtained, avoiding the difficulty of using traditional metal-catalyzed coupling reactions. To generate Csp<sup>3</sup> radicals, a number of chemical bonds (Csp<sup>3</sup>-Cl bonds, Csp<sup>3</sup>-Br bonds, Csp<sup>3</sup>-C bonds, Csp<sup>3</sup>-O bonds, *etc.*) have flexibly participated in redox-neutral coupling reactions and reductive cross-coupling reactions in the past five years. In some specific transformations, coupling reactions have been developed that do not require additional photocatalysts or ligands. However, most coupling reactions are driven by blue

LED light, and very few reactions are driven by purple light. In addition, the stereo- and regio-selectivities of these reactions still need further study.

In the next stage, we anticipate that the development trend of the Csp<sup>3</sup>-Csp<sup>3</sup> coupling reaction in Ni/photoredox dual catalysis may have the following six aspects: (a) recently, the asymmetric version of this field has experienced significant development.<sup>30</sup> It is believed that more efforts will be devoted to exploring asymmetric Csp<sup>3</sup>-Csp<sup>3</sup> coupling reactions by introducing chiral ligands into the catalytic system; (b) the mechanisms of some specific related reactions will be further clarified. Some new mechanisms will also emerge and become increasingly clear; (c) the formation method of C-centered sp<sup>3</sup> hybridized radicals that can participate in Csp<sup>3</sup>-Csp<sup>3</sup> cross-coupling reactions will be further expanded; (d) more classic conventional coupling reactions may be extended and also participate in the photo-nickel synergistic catalytic system to enable the formation of Csp<sup>3</sup>-Csp<sup>3</sup> structures; (e) site-selective Csp<sup>3</sup> alkylation *via* Csp<sup>3</sup>-Csp<sup>3</sup> cross-coupling reactions of dual photoredox/Ni-catalysis is another important direction and requires future development. We believe that the challenges in this area will eventually be overcome and more efficient, green, and gentle methods will be developed. (f) More types of light sources (such as red and green light) may be used in Csp<sup>3</sup>-Csp<sup>3</sup> cross-coupling reactions in the near future.

## Author contributions

Shi, M. directed the perspective and revised the manuscript. Huang, Q. Y. carried out the literature collection, organization, wrote the manuscript, drew the schemes and reviewed them.

## Data availability

No primary research results, software or code have been included and no new data were generated or analysed as part of this review.

## Conflicts of interest

There are no conflicts to declare.

## Acknowledgements

We are grateful for the financial support from the National Key R&D Program of China (2023YFA1506700), the National Natural Science Foundation of China (21372250, 21121062, 21302203, 20732008, 21772037, 21772226, 21861132014, 91956115 and 22171078), a project supported by the Shanghai Municipal Science and Technology Major Project (Grant No. 2018SHZDZX03) and the Fundamental Research Funds for the Central Universities 222201717003.



## References

- (a) S. Bhakta and T. Ghosh, Nickel-catalyzed hydroarylation reaction: a useful tool in organic synthesis, *Org. Chem. Front.*, 2022, **9**, 5074–5103; (b) S. Zhu, H. Li, Y. Li, Z. Huang and L. Chu, Exploring visible light for carbon–nitrogen and carbon–oxygen bond formation via nickel catalysis, *Org. Chem. Front.*, 2023, **10**, 548–569; (c) J. A. Milligan, J. P. Phelan, S. O. Badir and G. A. Molander, Alkyl Carbon–Carbon Bond Formation by Nickel/Photoredox Cross-Coupling, *Angew. Chem., Int. Ed.*, 2019, **58**, 6152–6163; (d) P. P. Singh, P. K. Singh and V. Srivastava, Visible light metallaphotoredox catalysis in the late-stage functionalization of pharmaceutically potent compounds, *Org. Chem. Front.*, 2023, **10**, 216–236.
- W. Yuan, S. Zheng and Y. Hu, Recent Advances in C(sp<sup>3</sup>)–C(sp<sup>3</sup>) Cross-Coupling via Metalla-photoredox Strategies, *Synthesis*, 2021, **53**, 1719–1733.
- J. Choi and G. C. Fu, Transition metal-catalyzed alkyl-alkyl bond formation: Another dimension in cross-coupling chemistry, *Science*, 2017, **356**, eaaf7230.
- (a) V. M. Chernyshev and V. P. Ananikov, Nickel and Palladium Catalysis: Stronger Demand than Ever, *ACS Catal.*, 2022, **12**, 1180–1200; (b) S. Z. Tasker, E. A. Standley and T. F. Jamison, Recent advances in homogeneous nickel catalysis, *Nature*, 2014, **509**, 299–309; (c) V. P. Ananikov, Nickel: The “Spirited Horse” of Transition Metal Catalysis, *ACS Catal.*, 2015, **5**, 1964–1971; (d) S. Crespi and M. Fagnoni, Generation of Alkyl Radicals: From the Tyranny of Tin to the Photon Democracy, *Chem. Rev.*, 2020, **120**, 9790–9833; (e) W. M. Cheng and R. Shang, Transition Metal-Catalyzed Organic Reactions under Visible Light: Recent Developments and Future Perspectives, *ACS Catal.*, 2020, **10**, 9170–9196; (f) K. L. Skubi, T. R. Blum and T. P. Yoon, Dual Catalysis Strategies in Photochemical Synthesis, *Chem. Rev.*, 2016, **116**, 10035–10074.
- (a) C. G. Dong and Q. S. Hu, Ni(cod)<sub>2</sub>/PCy<sub>3</sub>-Catalyzed Cross-Coupling Reactions of Dihaloarenes with Arylboronic Acids, *Synlett*, 2012, **23**, 2121–2125; (b) L. Cheng and Q. L. Zhou, Advances on Nickel-Catalyzed C(sp<sup>3</sup>)–C(sp<sup>3</sup>) Bond Formation, *Acta Chim. Sin.*, 2020, **78**, 1017–1029; (c) M. D. Levin, S. Kim and F. D. Toste, Photoredox Catalysis Unlocks Single-Electron Elementary Steps in Transition Metal Catalyzed Cross-Coupling, *ACS Cent. Sci.*, 2016, **2**, 293–301.
- (a) L. J. Goossen, F. Collet and K. Goossen, Decarboxylative Coupling Reactions, *Isr. J. Chem.*, 2010, **50**, 617–629; (b) Q. Zhao and M. Szostak, Redox-Neutral Decarboxylative Cross-Couplings Coming of Age, *ChemSusChem*, 2019, **12**, 2983–2987; (c) J. Xie, H. Jin and A. S. K. Hashmi, The recent achievements of redox-neutral radical C–C cross-coupling enabled by visible-light, *Chem. Soc. Rev.*, 2017, **46**, 5193–5203.
- L. Zhang, X. Si, Y. Yang, M. Zimmer, S. Witzel, K. Sekine, M. Rudolph and A. S. K. Hashmi, The Combination of Benzaldehyde and Nickel-Catalyzed Photoredox C(sp<sup>3</sup>)–H Alkylation/Arylation, *Angew. Chem., Int. Ed.*, 2019, **58**, 1823–1827.
- E. M. Dauncey, S. U. Dighe, J. J. Douglas and D. Leonori, A dual photoredox-nickel strategy for remote functionalization via iminyl radicals: radical ring-opening-arylation, -vinylation and -alkylation cascades, *Chem. Sci.*, 2019, **10**, 7728–7733.
- Y. Luo, A. Gutierrez-Bonet, J. K. Matsui, M. E. Rotella, R. Dykstra, O. Gutierrez and G. A. Molander, Oxa- and Azabenzonornbornadienes as Electrophilic Partners under Photoredox/Nickel Dual Catalysis, *ACS Catal.*, 2019, **9**, 8835–8842.
- M. S. Santos, A. G. Corrêa, M. W. Paixão and B. König, C(sp<sup>3</sup>)–C(sp<sup>3</sup>) Cross-Coupling of Alkyl Bromides and Ethers Mediated by Metal and Visible Light Photoredox Catalysis, *Adv. Synth. Catal.*, 2020, **362**, 2367–2372.
- M. B. Buendia, B. Higginson, S. Kegnæs, S. Kramer and R. Martin, Redox-Neutral Ni-Catalyzed sp<sup>3</sup> C–H Alkylation of  $\alpha$ -Olefins with Unactivated Alkyl Bromides, *ACS Catal.*, 2022, **12**, 3815–3820.
- H. A. Sakai and D. W. C. MacMillan, Nontraditional Fragment Couplings of Alcohols and Carboxylic Acids: C(sp<sup>3</sup>)–C(sp<sup>3</sup>) Cross-Coupling via Radical Sorting, *J. Am. Chem. Soc.*, 2022, **144**, 6185–6192.
- X. Y. Lv, R. Abrams and R. Martin, Dihydroquinazolinones as adaptative C(sp<sup>3</sup>) handles in arylations and alkylations via dual catalytic C–C bond-functionalization, *Nat. Commun.*, 2022, **13**, 2394.
- J. Zheng, C. Nopper, R. Bibi, A. Nikbakht, F. Bauer and B. Breit, Regio- and Diastereoselective Decarboxylative Allylation of *N*-Aryl  $\alpha$ -Amino Acids by Dual Photoredox/Nickel Catalysis, *ACS Catal.*, 2022, **12**, 5949–5960.
- S. Dongbang and A. G. Doyle, Ni/Photoredox-Catalyzed C(sp<sup>3</sup>)–C(sp<sup>3</sup>) Coupling between Aziridines and Acetals as Alcohol-Derived Alkyl Radical Precursors, *J. Am. Chem. Soc.*, 2022, **144**, 20067–20077.
- E. Mao and D. W. C. MacMillan, Late-Stage C(sp<sup>3</sup>)–H Methylation of Drug Molecules, *J. Am. Chem. Soc.*, 2023, **145**, 2787–2793.
- W. L. Lyon and D. W. C. MacMillan, Expedient Access to Underexplored Chemical Space: Deoxygenative C(sp<sup>3</sup>)–C(sp<sup>3</sup>) Cross-Coupling, *J. Am. Chem. Soc.*, 2023, **145**, 7736–7742.
- W. Wang, X. Yan, F. Ye, S. Zheng, G. Huang and W. Yuan, Nickel/Photoredox Dual-Catalyzed Regiodivergent Aminoalkylation of Unactivated Alkyl Halides, *J. Am. Chem. Soc.*, 2023, **145**, 23385–23394.
- B. Yang, X. Y. Wang, X. T. Huang, Z. Y. Liu, X. Li, T. Huang, X. S. Li, L. Z. Wu, R. Fang and Q. Liu, Visible-Light-Mediated Two Transient C(sp<sup>3</sup>) Radical-Selective Cross-Coupling via Nickel Catalyst Continuous Capture: Synthesis of Pyrroline Derivatives, *ACS Catal.*, 2023, **13**, 15331–15339.
- Z. Zhou, J. Yang, B. Yang, Y. Han, L. Zhu, X. S. Xue and F. Zhu, Photoredox Nickel-Catalysed Stille Cross-Coupling Reactions, *Angew. Chem., Int. Ed.*, 2023, **62**, e202314832.





- 21 Z. Hu, D. Wang and T. Xu, Direct Synthesis of  $\beta$ -Amino Boronates via Amide  $\alpha$ -C–H Bond Activation and C(sp<sup>3</sup>)–C(sp<sup>3</sup>) Coupling under Dual Ni/Photoredox Catalysis, *ACS Catal.*, 2024, **14**, 547–553.
- 22 (a) W. Zhang, J. Chen, H. Wei and L. Wu, Development of Nickel-Catalyzed Cross-Coupling of Alcohol Derivatives to Construct Carbon-Carbon Bonds, *Chin. J. Org. Chem.*, 2021, **41**, 4208–4239; (b) J. D. Sieber and T. Agrawal, *Synthesis*, 2020, **52**, 2623–2638; (c) S. Geng, C. Shi, B. Guo, H. Hou, Z. Liu and Z. Feng, Recent Progress in Transition-Metal-Catalyzed Reductive Cross-Coupling Reactions Using Diboron Reagents as Reductants, *ACS Catal.*, 2023, **13**, 15469–15480; (d) H. Wang and T. Xu, Dual nickel- and photoredox-catalyzed carbon-carbon bond formations via reductive cross-coupling involving organohalides, *Chem Catal.*, 2024, **4**, 100952.
- 23 F. Cong, X. Y. Lv, C. S. Day and R. Martin, Dual Catalytic Strategy for Forging sp<sup>2</sup>–sp<sup>3</sup> and sp<sup>3</sup>–sp<sup>3</sup> Architectures via  $\beta$ -Scission of Aliphatic Alcohol Derivatives, *J. Am. Chem. Soc.*, 2020, **142**, 20594–20599.
- 24 T. Yang, Y. Wei and M. J. Koh, Photoinduced Nickel-Catalyzed Deaminative Cross-Electrophile Coupling for C(sp<sup>2</sup>)–C(sp<sup>3</sup>) and C(sp<sup>3</sup>)–C(sp<sup>3</sup>) Bond Formation, *ACS Catal.*, 2021, **11**, 6519–6525.
- 25 S. K. Jana, M. Maiti, P. Dey and B. Maji, Photoredox/Nickel Dual Catalysis Enables the Synthesis of Alkyl Cyclopropanes via C(sp<sup>3</sup>)–C(sp<sup>3</sup>) Cross Electrophile Coupling of Unactivated Alkyl Electrophiles, *Org. Lett.*, 2022, **24**, 1298–1302.
- 26 Y. Xu, M. L. Zhang and M. Oestreich, Photochemical, Nickel-Catalyzed C(sp<sup>3</sup>)–C(sp<sup>3</sup>) Reductive Cross-Coupling of  $\alpha$ -Silylated Alkyl Electrophiles and Allylic Sulfones, *ACS Catal.*, 2022, **12**, 10546–10550.
- 27 J. Zhou, D. Wang, W. Xu, Z. Hu and T. Xu, Enantioselective C(sp<sup>3</sup>)–C(sp<sup>3</sup>) Reductive Cross-Electrophile Coupling of Unactivated Alkyl Halides with  $\alpha$ -Chloroboronates via Dual Nickel/Photoredox Catalysis, *J. Am. Chem. Soc.*, 2023, **145**, 2081–2087.
- 28 (a) Z. Huang, S. Tang and A. Lei, *Sci. Bull.*, 2015, **60**, 1391–1394; (b) C. Liu, D. Liu and A. Lei, *Acc. Chem. Res.*, 2014, **47**, 3459–3470; (c) I. Funes-Ardoiz and F. Maseras, *ACS Catal.*, 2018, **8**, 1161–1172; (d) Z. Yang, W. Shi, H. Alhumade, H. Yi and A. Lei, *Nat. Synth.*, 2023, **2**, 217–230.
- 29 A. V. Tsymbal, L. D. Bizzini and D. W. C. MacMillan, Nickel Catalysis via S<sub>H</sub>2 Homolytic Substitution: The Double Decarboxylative Cross-Coupling of Aliphatic Acids, *J. Am. Chem. Soc.*, 2022, **144**, 21278–21286.
- 30 J. Li, B. Cheng, X. Shu, Z. Xu, C. Li and H. Huo, Enantioselective alkylation of  $\alpha$ -amino C(sp<sup>3</sup>)–H bonds via photoredox and nickel catalysis, *Nat. Catal.*, 2024, DOI: [10.1038/s41929-024-01192-7](https://doi.org/10.1038/s41929-024-01192-7).

